

Annihilating to the Darker: A Cure for WIMP

Wan-Zhe Feng* and Zi-Hui Zhang†

Center for Joint Quantum Studies and Department of Physics,
School of Science, Tianjin University, Tianjin 300350, P.R. China

(Dated: October 3, 2024)

We propose that the non-observation of WIMPs may be explained by dark matter primarily *annihilating to the darker* concealed sector while coupling to the standard model with only minimal strength. To demonstrate this scenario, we focus on the WIMP dark matter candidate from a $U(1)_x$ hidden sector, which couples more strongly to another concealed $U(1)_c$ sector than to the standard model. We explore two possible cases for the evolution of dark particles among hidden sectors: (1) The WIMP annihilates efficiently and achieves the observed relic density with the assistance of the concealed sector. (2) The WIMP transforms into another type of dark matter within the concealed sector and attains the observed relic density. *Annihilating to the darker* explains why WIMPs have remained undetected, and all WIMP models will continue to hold interest.

Introduction.—The null detection of weakly interacting massive particle (WIMP) as dark matter candidate has placed significant strain on a large number of dark matter models. The increased intensity and precision of probes into dark matter through various direct [1–6] and indirect [7–10] detection experiments significantly narrow down the parameter space for majority of WIMP dark matter models. The reason is remarkably straightforward: to achieve a sufficiently large annihilation cross-section capable of reducing the amount of dark matter to match the observed relic density, the couplings of dark matter to Standard Model particles must inevitably be large. This leads to substantial elastic scattering cross-sections between the dark matter and hadrons which have been already excluded by direct detection experiments.[31] Additionally, the same large dark matter annihilation cross-sections also produce noticeable indirect detection signals for dark matter, which as well haven’t yet been detected.

It is widely accepted that dark matter resides in one or multiple hidden sectors, which exist generally in various GUT models and string theory. Since dark matter hasn’t been detected other than gravitational observations, it is possible that dark matter undergoes strong interactions within multiple hidden sectors, while only ultraweakly coupled to the Standard Model. Thus in this new era of dark matter research, it is essential to explore interactions among multiple hidden sectors that contain dark matter candidates.[32]

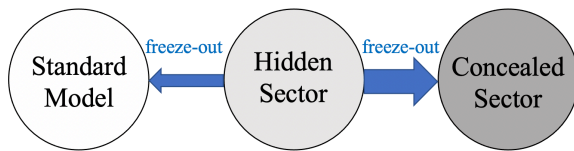


FIG. 1. *Annihilating to the darker*: WIMPs from the hidden sector primarily freezes out into a darker concealed sector rather than into the Standard Model.

In this letter, we explore a novel framework in which the WIMP resides within the first hidden sector, strongly interacts with another concealed sector that is more weakly coupled to the Standard Model, making it “darker”. Thus the WIMP primarily annihilates into this darker concealed sector rather than into the Standard Model, as illustrated in Fig. 1. The WIMP exhibits relatively modest couplings with Standard Model particles, and is hence not yet discovered by direct detection experiments under the current sensitivity. We investigate two distinct possibilities:

- **Case 1:** The WIMP from the hidden sector mainly freezes out into the concealed sector, yielding a relic density of approximately 0.12. Particles within the concealed sector consequently decay or annihilate to Standard Model particles, resulting in their eventual disappearance in the Universe.
- **Case 2:** The WIMP from the hidden sector primarily freezes out into the concealed sector, leaving only a subdominant portion, while particles in the concealed sector constitute the majority of the dark matter.

Annihilating to the darker is broadly applicable and may explain why *all* WIMP models have remained undetected. The core concept is straightforward and holds the potential to revitalize various WIMP models previously considered obsolete, aligning with this paradigm.

The model.—For simplicity and concreteness, we focus on the dark matter candidate as a $U(1)_x$ charged fermion χ_x residing in a $U(1)_x$ hidden sector, with its mass situated in the traditional WIMP region, i.e., 1 – 200 GeV. The dark matter χ_x freezes out into Standard Model particles but predominantly into the concealed $U(1)_c$ sector, due to the $U(1)_x$ sector coupling more strongly to $U(1)_c$, shown in Fig. 2. Also for simplicity, we discuss the dark $U(1)$ gauge bosons achieving mass via Stueckelberg mechanism [16]. The case of dark Higgs fields breaking the dark $U(1)$ symmetries can be treated in the

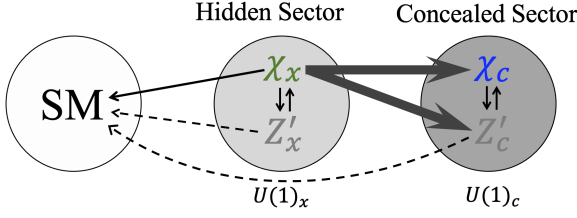


FIG. 2. A Graphic illustration of a two- $U(1)$ model. The WIMP dark matter χ_x primarily freezes out to χ_c and Z'_c from the darker concealed $U(1)_c$ sector, while only a small fraction freezes out into Standard Model particles. In Case 1, $\Omega_{\chi_x} h^2 \sim 0.12$, and χ_c is subdominant. In Case 2, χ_x mainly transforms to χ_c with $\Omega_{\chi_c} h^2 \sim 0.12$.

same way. In the unitary gauge, one has $U(1)_x$ gauge boson X_μ with mass set larger than the mass of χ_x . [33]

We focus on the case that all of Standard Model particles are not charged under $U(1)_x$, and the $U(1)_x$ sector connects with the Standard Model via kinetic mixing [18] and/or mass mixing [19–21]. In this case the $U(1)_x$ gauge coupling can be substantial while the mixing parameters must remain small.

The total effective Lagrangian of the model is given by

$$\mathcal{L} = \mathcal{L}_{\text{SM}} + \mathcal{L}_{\text{hid}} + \mathcal{L}_{\text{con}} + \mathcal{L}_{\text{mix}}, \quad (1)$$

where \mathcal{L}_{hid} , \mathcal{L}_{con} , \mathcal{L}_{mix} are given by

$$\mathcal{L}_{\text{hid}} = -\frac{1}{4}F_{x\mu\nu}F_x^{\mu\nu} + g_x X_\mu \bar{\chi}_x \gamma^\mu \chi_x - m_x \bar{\chi}_x \chi_x - \frac{1}{2}M_x^2 X_\mu^2 \quad (2)$$

$$\mathcal{L}_{\text{con}} = -\frac{1}{4}F_{c\mu\nu}F_c^{\mu\nu} + g_c C_\mu \bar{\chi}_c \gamma^\mu \chi_c - m_c \bar{\chi}_c \chi_c - \frac{1}{2}M_c^2 C_\mu^2 \quad (3)$$

$$\mathcal{L}_{\text{mix}} = -\frac{\delta_1}{2}F_{x\mu\nu}F_Y^{\mu\nu} - \frac{\delta_2}{2}F_{x\mu\nu}F_c^{\mu\nu} - \frac{1}{2}M_m^2 X_\mu C^\mu, \quad (4)$$

where the dark fermion $\chi_x(\chi_c)$ is charged +1 under $U(1)_x(U(1)_c)$, $\delta_1(\delta_2)$ is the kinetic mixing parameter for $U(1)_x$ and $U(1)_Y(U(1)_c)$ and $\delta_2 \gg \delta_1$. Mass mixing is common among multiple hidden sectors and can be generated through either the dark Higgs or Stueckelberg mechanism, characterized by the parameter M_m in Eq. (4). Especially, the mass mixing has well-motivated string theory origin [22], see [23] for a general discussion.

Now we rewrite the Lagrangian in the gauge eigenbasis $V^T = (C, X, B, A^3)$, with the kinetic mixing matrix and mass mixing matrix given by

$$\mathcal{K} = \begin{pmatrix} 1 & \delta_2 & 0 & 0 \\ \delta_2 & 1 & \delta_1 & 0 \\ 0 & \delta_1 & 1 & 0 \\ 0 & 0 & 0 & 1 \end{pmatrix}, \quad (5)$$

$$\mathbf{M}^2 = \begin{pmatrix} M_c^2 & M_m^2 & & \\ M_m^2 & M_x^2 & & 0 \\ 0 & & -\frac{1}{4}v^2 g_Y^2 & -\frac{1}{4}v^2 g_2 g_Y \\ 0 & & -\frac{1}{4}v^2 g_2 g_Y & \frac{1}{4}v^2 g_2^2 \end{pmatrix}. \quad (6)$$

To obtain the couplings of the physical gauge bosons with fermions, a simultaneous diagonalization of both the kinetic and mass mixing matrices brings the original basis into physical mass eigenbasis $E^T = (Z'_c, Z'_x, A_\gamma, Z)$ with a 4×4 rotation matrix \mathcal{R} such that $V = \mathcal{R}E$.

The interactions between gauge bosons and fermions can be determined from

$$\mathcal{L}_{\text{int}} = (g_c J_c, g_x J_x, g_Y J_Y, g_2 J_3) \mathcal{R}E, \quad (7)$$

where J_Y, J_3, J_x, J_c are the hypercharge current, the $SU(2)$ neutral current and the $U(1)_x, U(1)_c$ dark current respectively

$$J_c^\mu = \bar{\chi}_c \gamma^\mu \chi_c, \quad J_x^\mu = \bar{\chi}_x \gamma^\mu \chi_x, \quad J_3^\mu = T_i^3 \bar{f}_i \gamma^\mu P_L f_i, \quad (8)$$

$$J_Y^\mu = Y_{i_L} \bar{f}_i \gamma^\mu P_L f_i + Y_{i_R} \bar{f}_i \gamma^\mu P_R f_i. \quad (9)$$

The coupling of the $U(1)_x$ sector to the Standard Model is of the order of $g_x \delta_1$, which is set by both the dark matter direct detection and collider constraints. The couplings of the $U(1)_c$ sector to the Standard Model are weaker due to the indirect mixing effect.

In addition to the conventional dark matter annihilation channels to Standard Model fermions ($\chi_x \bar{\chi}_x \rightarrow f_i \bar{f}_i$), [34] which are insufficient to deplete the abundance of χ_x , new annihilation channels to the concealed sector $\chi_x \bar{\chi}_x \rightarrow \chi_c \bar{\chi}_c, Z'_c Z'_c, Z'_c Z'_c, Z Z'_c$ significantly reduce χ_x abundance down to the observed relic density value. Gauge bosons Z'_x, Z'_c decay into Standard Model fermions prior to Big Bang nucleosynthesis.

The full Boltzmann equations which govern the evolution of all dark particles are given in the Appendix.

Experimental constraints.—The most stringent constraints on 1–200 GeV dark matter arise from direct detection experiments and collider data.

Direct detection constraints The spin-independent cross-section for dark matter scattering off a nucleon is given by

$$\sigma_p^{\text{SI}} = \frac{\mu_p^2 [Z f_p + (A - Z) f_n]^2}{\pi A^2}, \quad (10)$$

where A, Z are the mass number and atomic number respectively, $\mu_p = m_p m_\chi / (m_p + m_\chi)$ is the WIMP-proton reduced mass. The effective WIMP couplings to protons and neutrons f_p, f_n are given by the quark effective couplings $f_p = 2f_u + f_d, f_n = f_u + 2f_d$, and are calculated from the effective operators

$$\mathcal{L}_{\text{eff}}^u = f_u \bar{\chi} \gamma_\mu \chi \bar{u} \gamma^\mu u, \quad \mathcal{L}_{\text{eff}}^d = f_d \bar{\chi} \gamma_\mu \chi \bar{d} \gamma^\mu d, \quad (11)$$

where the effective couplings are given by

$$f_u = \sum_a \frac{g_{\chi a} (g_{uLa} + g_{uRa})}{2M_a^2}, \quad f_d = \sum_a \frac{g_{\chi a} (g_{dLa} + g_{dRa})}{2M_a^2}. \quad (12)$$

In the above expressions, g_{ia} represents the coupling of gauge bosons $a = Z, Z'_x, Z'_c$ to fermion and anti-fermion

pairs $\bar{i}i$ where $i = \chi_x, \chi_c, u_L, u_R, d_L, d_R$. Both χ_x from $U(1)_x$ sector and χ_c from $U(1)_c$ sector are dark matter candidates and are thus subject to the direct detection constraints. In the WIMP mass range under consideration, direct detection experiments [1–6] impose the most stringent constraints on the model.

Indirect detection constraints The main constraint on indirect detection of stable dark matter arises from its annihilation to Standard Model particles. In the analysis we used constraints from CMB [7], AMS02 [8], *Fermi* [9] and CTA [10] for various Standard Model final states. Dark matter annihilating into hidden sectors is also restricted by $\chi\bar{\chi} \rightarrow Z'Z' \rightarrow \text{SM}$ processes for $U(1)$ models [24]. We find that in the WIMP mass region, indirect detection constraints are not significant compared with direct detection and collider constraints.

Collider constraints The Z' boson can be produced at hadron colliders through the Drell-Yan process and detected as a resonance in the final state dilepton invariant mass spectrum. The ATLAS and CMS collaborations provide the most sensitive searches for Z' decays into the dilepton final state [25, 26]. We obtain the collider constraints for the $U(1)_x$ gauge boson by rescaling the collider limits of the Sequential Standard Model gauge boson Z'_{SSM} [27].

Benchmark models and Phenomenology.—After carefully solving the coupled Boltzmann equations detailed in the Appendix to trace the evolution of all dark particles, we present benchmark models for Case 1 ($\Omega_{\chi_x} h^2 \sim 0.12$) and Case 2 ($\Omega_{\chi_c} h^2 \sim 0.12$) in Tables I and II respectively (all masses are in units of GeV). Parameters are chosen to satisfy all current experimental constraints, especially ensuring that dark matter-nucleon spin-independent cross-sections are one order of magnitude below the strictest existing limits.

For Case 1, although χ_x couples ultraweakly with the Standard Model particles, it annihilates efficiently with the assistance of the $U(1)_c$ sector. In this case, depleting χ_x sufficiently requires only a $U(1)_c$ gauge boson, and χ_c is not necessary for the model, though it is retained for a more comprehensive discussion. We present Models 1a – 1d, 1d' for Case 1, which feature both kinetic and mass mixing between $U(1)_x$ and $U(1)_c$, characterized by δ_2 and M_m respectively. We highlight that pure kinetic mixing, with M_m set to zero, is fully effective for all cases.

Model 1d' holds special interest since asymmetric dark matter models typically predict an $\mathcal{O}(1)$ GeV dark matter particle to explain the cosmic coincidence puzzle [28–30]. To ensure that the asymmetric component constitutes the majority of dark matter, the symmetric portion must undergo further freeze-out to constitute less than 10% of the total dark matter relic density. Using the mechanism described in the letter, the symmetric portion in Model 1d' is readily depleted to 10%.

For Case 2, χ_x primarily freezes out into the $U(1)_c$ sector and transforms into χ_c , becoming the dominant dark

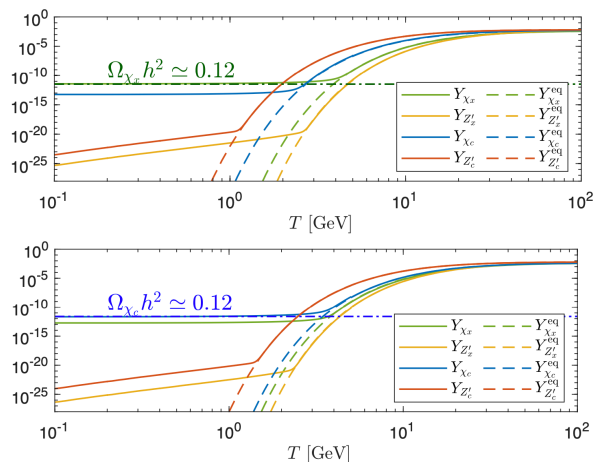


FIG. 3. Evolution of dark particles in Models 1b (above) and 2b (below), both including a 100 GeV WIMP χ_x that primarily annihilates to the concealed sector. In model 1b, χ_x is the dominant dark matter candidate whereas in model 2b, χ_c constitutes the majority of the dark matter.

matter candidate, while χ_x leaves only a subdominant portion. In Table II, we show two types of benchmarks, both include kinetic and mass mixing. Models 2c' and 2d' represent a specific type of models where the dark matter χ_c is the lightest among the entire hidden sector.

Fig. 3 illustrates the evolution of dark particles for Models 1b and 2b, both featuring an undetected 100 GeV WIMP χ_x . In Model 1b, χ_x depletes efficiently and serves as the primary dark matter candidate, while in Model 2b χ_c becomes the dominant dark matter candidate.

Conclusion.—WIMP is one of the most extensively studied dark matter candidates in history. The non-observation of WIMPs in direct detection experiments poses a significant threat to numerous WIMP models. In this letter, we discuss the possibility that the absence of WIMP discoveries may be attributed to more complex interactions among hidden sectors beyond the Standard Model. Dark matter couples to another concealed sector with much larger strength than it does to the Standard Model sector. Thus, in addition to freezing out into Standard Model particles with only a small fraction, which may still provide direct detection signals for future experiments, most thermal WIMPs predominantly annihilate into a darker concealed sector, as illustrated in Fig. 1. This scenario is demonstrated by a simple two- $U(1)$ model depicted in Fig. 2. Two distinct cases have been investigated with the WIMP either depletes efficiently into the concealed sector or transforms to another form of dark matter within the concealed sector. We propose that many nearly excluded WIMP models remain of interest since the dark matter is primarily *annihilating to the darker* concealed sector and continue to hold potential for future dark matter detections.

Model	m_x	m_c	M_x	M_c	M_m	$M_{Z'_x}$	$M_{Z'_c}$	δ_1	δ_2	g_x	g_c	$\Omega_{\chi_x} h^2$	$\Omega_{\chi_c} h^2$
1a	200	90	210	80	100	211	65	1×10^{-4}	0.15	0.525	0.6	0.12	7.5×10^{-3}
1b	100	70	120	60	60	121	51.5	3×10^{-5}	0.1	0.4	0.6	0.12	2.0×10^{-3}
1c	10	6	15	4	3	15	4	6×10^{-6}	0.05	0.14	0.6	0.12	7.7×10^{-4}
1d	1	0.5	1.6	0.3	0.3	1.6	0.3	1×10^{-4}	0.01	0.055	0.4	0.12	1.5×10^{-4}
1d'	1	0.5	1.6	0.3	0.3	1.6	0.3	1×10^{-4}	0.01	0.17	0.4	0.012	4.9×10^{-5}

TABLE I. Case 1 benchmark models: The WIMP dark matter χ_x mainly freezes out into the concealed sector, and remains undetected. Model 1d' demonstrates that models with $\mathcal{O}(1)$ GeV asymmetric dark matter candidates can efficiently reduce the symmetric portion to less than 10% under the mechanism described in this letter.

Model	m_x	m_c	M_x	M_c	M_m	$M_{Z'_x}$	$M_{Z'_c}$	δ_1	δ_2	g_x	g_c	$\Omega_{\chi_x} h^2$	$\Omega_{\chi_c} h^2$
2a	200	165	210	160	160	221	103	4×10^{-5}	0.3	0.6	0.31	0.017	0.103
2b	100	90	110	80	70	112	67	2×10^{-5}	0.2	0.6	0.235	0.010	0.11
2c	10	7	12	6.5	5	12	6.3	1×10^{-6}	0.2	0.6	0.075	1.5×10^{-3}	0.12
2d	1	0.5	1.6	0.3	0.3	1.6	0.3	1×10^{-4}	0.1	0.6	0.02	6.3×10^{-4}	0.12
2c'	10	7	12	9	5.8	12.6	8.2	1×10^{-6}	0.005	0.6	0.6	8.5×10^{-4}	0.12
2d'	1	0.65	1.2	0.82	0.3	1.2	0.81	1×10^{-4}	0.001	0.5	0.46	3.0×10^{-4}	0.12

TABLE II. Case 2 benchmark models: The WIMP dark matter χ_x primarily freezes out into the concealed sector, converting to χ_c , the dominant dark matter candidate, and leaving only a small fraction remaining in the Universe. Models 2c' and 2d' represent a specific type of models where the dark matter candidate χ_c is the lightest particle in the entire hidden sector.

Acknowledgments This work is supported by the Na-

tional Natural Science Foundation of China under Grant No. 11935009.

Appendix.—The full Boltzmann equations are given by

$$\begin{aligned} \frac{dY_{\chi_x}}{dT} = & -\frac{s}{T\bar{H}} \sum_{i \in \text{SM}} \left\{ [(Y_{\chi_x}^{\text{eq}})^2 - Y_{\chi_x}^2] \langle \sigma v \rangle_{\chi_x \bar{\chi}_x \rightarrow f_i \bar{f}_i} \right. \\ & + Y_{\chi_c}^2 \langle \sigma v \rangle_{\chi_c \bar{\chi}_c \rightarrow \chi_x \bar{\chi}_x} - Y_{\chi_x}^2 \langle \sigma v \rangle_{\chi_x \bar{\chi}_x \rightarrow \chi_c \bar{\chi}_c} \\ & + Y_{Z'_x}^2 \langle \sigma v \rangle_{Z'_x Z'_x \rightarrow \chi_x \bar{\chi}_x} - Y_{\chi_x}^2 \langle \sigma v \rangle_{\chi_x \bar{\chi}_x \rightarrow Z'_x Z'_x} \\ & + Y_{Z'_c}^2 \langle \sigma v \rangle_{Z'_c Z'_c \rightarrow \chi_x \bar{\chi}_x} - Y_{\chi_x}^2 \langle \sigma v \rangle_{\chi_x \bar{\chi}_x \rightarrow Z'_c Z'_c} \\ & \left. + Y_{Z'_x} Y_{Z'_c} \langle \sigma v \rangle_{Z'_x Z'_c \rightarrow \chi_x \bar{\chi}_x} - Y_{\chi_x}^2 \langle \sigma v \rangle_{\chi_x \bar{\chi}_x \rightarrow Z'_x Z'_c} \right\}, \end{aligned} \quad (13)$$

$$\begin{aligned} \frac{dY_{\chi_c}}{dT} = & -\frac{s}{T\bar{H}} \sum_{i \in \text{SM}} \left\{ [(Y_{\chi_c}^{\text{eq}})^2 - Y_{\chi_c}^2] \langle \sigma v \rangle_{\chi_c \bar{\chi}_c \rightarrow f_i \bar{f}_i} \right. \\ & - Y_{\chi_c}^2 \langle \sigma v \rangle_{\chi_c \bar{\chi}_c \rightarrow \chi_x \bar{\chi}_x} + Y_{\chi_x}^2 \langle \sigma v \rangle_{\chi_x \bar{\chi}_x \rightarrow \chi_c \bar{\chi}_c} \\ & + Y_{Z'_x}^2 \langle \sigma v \rangle_{Z'_x Z'_x \rightarrow \chi_c \bar{\chi}_c} - Y_{\chi_c}^2 \langle \sigma v \rangle_{\chi_c \bar{\chi}_c \rightarrow Z'_x Z'_x} \\ & + Y_{Z'_c}^2 \langle \sigma v \rangle_{Z'_c Z'_c \rightarrow \chi_c \bar{\chi}_c} - Y_{\chi_c}^2 \langle \sigma v \rangle_{\chi_c \bar{\chi}_c \rightarrow Z'_c Z'_c} \\ & \left. + Y_{Z'_x} Y_{Z'_c} \langle \sigma v \rangle_{Z'_x Z'_c \rightarrow \chi_c \bar{\chi}_c} - Y_{\chi_c}^2 \langle \sigma v \rangle_{\chi_c \bar{\chi}_c \rightarrow Z'_x Z'_c} \right\}, \end{aligned} \quad (14)$$

$$\begin{aligned} \frac{dY_{Z'_x}}{dT} = & -\frac{s}{T\bar{H}} \sum_{i \in \text{SM}} \left[Y_i^2 \langle \sigma v \rangle_{f_i \bar{f}_i \rightarrow Z'_x} - \frac{1}{s} Y_{Z'_x} \langle \Gamma \rangle_{Z'_x \rightarrow f_i \bar{f}_i} \right. \\ & \left. - Y_{Z'_x}^2 (\langle \sigma v \rangle_{Z'_x Z'_x \rightarrow \chi_x \bar{\chi}_x} + \langle \sigma v \rangle_{Z'_x Z'_x \rightarrow \chi_c \bar{\chi}_c}) \right] \end{aligned}$$

$$\begin{aligned} & + Y_{\chi_x}^2 \langle \sigma v \rangle_{\chi_x \bar{\chi}_x \rightarrow Z'_x Z'_x} + Y_{\chi_c}^2 \langle \sigma v \rangle_{\chi_c \bar{\chi}_c \rightarrow Z'_x Z'_x} \\ & - Y_{Z'_x} Y_{Z'_c} (\langle \sigma v \rangle_{Z'_x Z'_c \rightarrow \chi_x \bar{\chi}_x} + \langle \sigma v \rangle_{Z'_x Z'_c \rightarrow \chi_c \bar{\chi}_c}) \\ & \left. + Y_{\chi_x}^2 \langle \sigma v \rangle_{\chi_x \bar{\chi}_x \rightarrow Z'_x Z'_c} + Y_{\chi_c}^2 \langle \sigma v \rangle_{\chi_c \bar{\chi}_c \rightarrow Z'_x Z'_c} \right], \end{aligned} \quad (15)$$

$$\begin{aligned} \frac{dY_{Z'_c}}{dT} = & -\frac{s}{T\bar{H}} \sum_{i \in \text{SM}} \left[Y_i^2 \langle \sigma v \rangle_{f_i \bar{f}_i \rightarrow Z'_c} - \frac{1}{s} Y_{Z'_c} \langle \Gamma \rangle_{Z'_c \rightarrow f_i \bar{f}_i} \right. \\ & - Y_{Z'_c}^2 (\langle \sigma v \rangle_{Z'_c Z'_c \rightarrow \chi_x \bar{\chi}_x} + \langle \sigma v \rangle_{Z'_c Z'_c \rightarrow \chi_c \bar{\chi}_c}) \\ & + Y_{\chi_x}^2 \langle \sigma v \rangle_{\chi_x \bar{\chi}_x \rightarrow Z'_c Z'_c} + Y_{\chi_c}^2 \langle \sigma v \rangle_{\chi_c \bar{\chi}_c \rightarrow Z'_c Z'_c} \\ & - Y_{Z'_x} Y_{Z'_c} (\langle \sigma v \rangle_{Z'_x Z'_c \rightarrow \chi_x \bar{\chi}_x} + \langle \sigma v \rangle_{Z'_x Z'_c \rightarrow \chi_c \bar{\chi}_c}) \\ & \left. + Y_{\chi_x}^2 \langle \sigma v \rangle_{\chi_x \bar{\chi}_x \rightarrow Z'_x Z'_c} + Y_{\chi_c}^2 \langle \sigma v \rangle_{\chi_c \bar{\chi}_c \rightarrow Z'_x Z'_c} \right], \end{aligned} \quad (16)$$

where $s = \frac{2\pi^2}{45} h_{\text{eff}} T^3$ and

$$\bar{H} = \frac{H}{1 + \frac{1}{3} \frac{T}{h_{\text{eff}}} \frac{dh_{\text{eff}}}{dT}} = \sqrt{\frac{\pi^2 g_{\text{eff}}}{90}} \frac{T^2/M_{\text{Pl}}}{1 + \frac{1}{3} \frac{T}{h_{\text{eff}}} \frac{dh_{\text{eff}}}{dT}}. \quad (17)$$

-
- * vicf@tju.edu.cn
† zhangzh_@tju.edu.cn
- [1] E. Aprile *et al.* [XENON], Phys. Rev. Lett. **123**, no.24, 241803 (2019) doi:10.1103/PhysRevLett.123.241803 [arXiv:1907.12771 [hep-ex]].
- [2] E. Aprile *et al.* [XENON], Phys. Rev. Lett. **123**, no.25, 251801 (2019) doi:10.1103/PhysRevLett.123.251801 [arXiv:1907.11485 [hep-ex]].
- [3] P. Agnes *et al.* [DarkSide-50], Phys. Rev. D **107**, no.6, 6 (2023) doi:10.1103/PhysRevD.107.063001 [arXiv:2207.11966 [hep-ex]].
- [4] Y. Meng *et al.* [PandaX-4T], Phys. Rev. Lett. **127**, no.26, 261802 (2021) doi:10.1103/PhysRevLett.127.261802 [arXiv:2107.13438 [hep-ex]].
- [5] J. Aalbers *et al.* [LZ], Phys. Rev. Lett. **131**, no.4, 041002 (2023) doi:10.1103/PhysRevLett.131.041002 [arXiv:2207.03764 [hep-ex]].
- [6] E. Aprile *et al.* [XENON], Phys. Rev. Lett. **131**, no.4, 041003 (2023) doi:10.1103/PhysRevLett.131.041003 [arXiv:2303.14729 [hep-ex]].
- [7] P. A. R. Ade *et al.* [Planck], Astron. Astrophys. **594**, A13 (2016) doi:10.1051/0004-6361/201525830 [arXiv:1502.01589 [astro-ph.CO]].
- [8] M. Aguilar *et al.* [AMS], Phys. Rept. **894**, 1-116 (2021) doi:10.1016/j.physrep.2020.09.003
- [9] A. McDaniel, M. Ajello, C. M. Karwin, M. Di Mauro, A. Drlica-Wagner and M. A. Sánchez-Conde, Phys. Rev. D **109**, no.6, 063024 (2024) doi:10.1103/PhysRevD.109.063024 [arXiv:2311.04982 [astro-ph.HE]].
- [10] A. Acharyya *et al.* [CTA], JCAP **01**, 057 (2021) doi:10.1088/1475-7516/2021/01/057 [arXiv:2007.16129 [astro-ph.HE]].
- [11] A. Aboubrahim, W. Z. Feng, P. Nath and Z. Y. Wang, JHEP **06**, 086 (2021) doi:10.1007/JHEP06(2021)086 [arXiv:2103.15769 [hep-ph]].
- [12] A. Aboubrahim and P. Nath, JHEP **09**, 084 (2022) doi:10.1007/JHEP09(2022)084 [arXiv:2205.07316 [hep-ph]].
- [13] P. N. Bhattachin, R. McGehee and A. Pierce, Phys. Rev. D **110**, no.3, 3 (2024) doi:10.1103/PhysRevD.110.L031702 [arXiv:2312.14152 [hep-ph]].
- [14] W. Z. Feng and Z. H. Zhang, [arXiv:2405.19431 [hep-ph]].
- [15] P. N. Bhattachin, R. McGehee, E. Petrosky and A. Pierce, [arXiv:2408.07744 [hep-ph]].
- [16] B. Kors and P. Nath, Phys. Lett. B **586**, 366-372 (2004) doi:10.1016/j.physletb.2004.02.051 [arXiv:hep-ph/0402047 [hep-ph]].
- [17] M. Pospelov, A. Ritz and M. B. Voloshin, Phys. Lett. B **662**, 53-61 (2008) doi:10.1016/j.physletb.2008.02.052 [arXiv:0711.4866 [hep-ph]].
- [18] B. Holdom, Phys. Lett. B **166**, 196-198 (1986) doi:10.1016/0370-2693(86)91377-8
- [19] K. Cheung and T. C. Yuan, JHEP **03**, 120 (2007) doi:10.1088/1126-6708/2007/03/120 [arXiv:hep-ph/0701107 [hep-ph]].
- [20] D. Feldman, Z. Liu and P. Nath, Phys. Rev. D **75**, 115001 (2007) doi:10.1103/PhysRevD.75.115001 [arXiv:hep-ph/0702123 [hep-ph]].
- [21] W. Z. Feng, Z. H. Zhang and K. Y. Zhang, JCAP **05**, 112 (2024) doi:10.1088/1475-7516/2024/05/112 [arXiv:2312.03837 [hep-ph]].
- [22] W. Z. Feng, G. Shiu, P. Soler and F. Ye, JHEP **05**, 065 (2014) doi:10.1007/JHEP05(2014)065 [arXiv:1401.5890 [hep-ph]].
- [23] W. Z. Feng, G. Shiu, P. Soler and F. Ye, Phys. Rev. Lett. **113**, 061802 (2014) doi:10.1103/PhysRevLett.113.061802 [arXiv:1401.5880 [hep-ph]].
- [24] G. Elor, N. L. Rodd, T. R. Slatyer and W. Xue, JCAP **06**, 024 (2016) doi:10.1088/1475-7516/2016/06/024 [arXiv:1511.08787 [hep-ph]].
- [25] G. Aad *et al.* [ATLAS], Phys. Lett. B **796**, 68-87 (2019) doi:10.1016/j.physletb.2019.07.016 [arXiv:1903.06248 [hep-ex]].
- [26] A. M. Sirunyan *et al.* [CMS], JHEP **07**, 208 (2021) doi:10.1007/JHEP07(2021)208 [arXiv:2103.02708 [hep-ex]].
- [27] G. Altarelli, B. Mele and M. Ruiz-Altaba, Z. Phys. C **45**, 109 (1989) [erratum: Z. Phys. C **47**, 676 (1990)] doi:10.1007/BF01556677
- [28] D. E. Kaplan, M. A. Luty and K. M. Zurek, Phys. Rev. D **79**, 115016 (2009) doi:10.1103/PhysRevD.79.115016 [arXiv:0901.4117 [hep-ph]].
- [29] W. Z. Feng, P. Nath and G. Peim, Phys. Rev. D **85**, 115016 (2012) doi:10.1103/PhysRevD.85.115016 [arXiv:1204.5752 [hep-ph]].
- [30] W. Z. Feng and P. Nath, Phys. Lett. B **731**, 43-50 (2014) doi:10.1016/j.physletb.2014.02.020 [arXiv:1312.1334 [hep-ph]].
- [31] Unless one considers quark-phobic types of dark matter models, where dark matter does not annihilate into quarks. These types of models face minimal constraints from dark matter direct detection experiments. In this letter, we focus on dark matter models that are subject to stringent constraints from direct and indirect detections, as well as collider searches.
- [32] Previous research on multiple hidden sectors within the freeze-in scenario includes [11–15].
- [33] The WIMP χ_x will primarily annihilate into the $U(1)_x$ gauge boson X_μ if X_μ is lighter than χ_x [17].
- [34] We note that WIMP annihilation to Zh, W^+W^- final states is suppressed compared to annihilation into Standard Model fermion pairs, and thus we omit these contributions in the Boltzmann equations.